KECK SPECTROSCOPY OF THE HUBBLE DEEP FIELD

G.D ILLINGWORTH, J. GALLEGO, R. GUZMÁN, J.D. LOWENTHAL, A.C. PHILLIPS, N.P. VOGT, D.C. KOO & S.M. FABER
UCO/Lick Observatory, University of California, Santa Cruz, CA, 95064, USA

Spectra of 115 HDF galaxies to I $\sim$ 25 mag were obtained by the Santa Cruz DEEP group with the Keck LRIS multislit spectrograph and combined with detailed structural measurements from the HDF images to (i) derive evolution for a sample of disk galaxies at $z \sim 0.5$ using the Tully-Fisher relation, (ii) characterize, from size and velocity width data, the global properties to $z \sim 1$ of a sample of $\sim$60 "compact" galaxies, (iii) determine star formation rates in that "compact" sample, and (iv) derive structure and redshifts for a sample of U and B-band "dropout" objects, of which 11 have been confirmed to be at high redshift ($z = 2.2 - 3.5$).

1 DEEP

The DEEP Project[a] was developed with the goal of elucidating the physical processes and time scales of the formation and evolution of galaxies. The Keck telescopes and their multi-object spectrographs (LRIS and later DEIMOS) are central to this program. Of equal importance is the high spatial resolution imaging capability provided by HST and its WFPC2 camera (and NICMOS, plus the Advanced Camera, the ACS, in 1999). The structural and morphological information from wide-field HST imaging has revolutionized the study of distant galaxies. The importance of such HST-imaged regions for the study of galaxies at intermediate to high redshift cannot be overstated. Ground-based telescopes, even with adaptive optical systems, will not provide comparable capability for the foreseeable future.

2 HDF Results

For a specific example of the importance of HST for clarifying the nature of galaxies in the young universe, one needs only to think of the impact of the Hubble Deep Field (Williams *et al.* 1996), and of the projects that the HDF images have precipitated.

The first results from the DEEP team's Keck LRIS observations of the HDF and its flanking fields are available in four papers, and are summarized below. The results are based on samples of galaxies selected from the HDF to meet a number of scientific goals. Structural parameters, colors, surface brightnesses

[a]Deep Extragalactic Evolutionary Probe; for further information see the DEEP home page at http://www.ucolick.org/ deep/home.html.

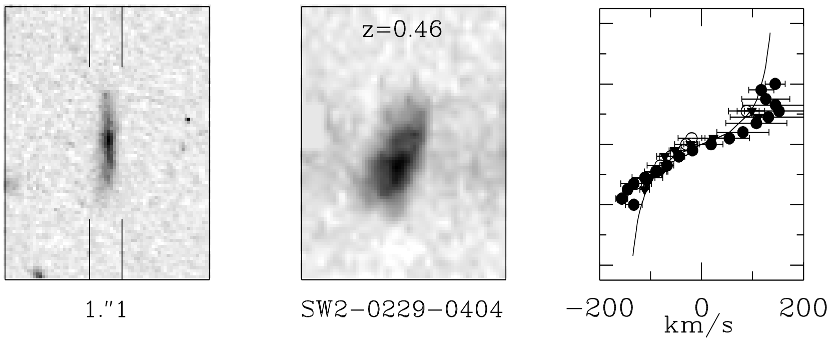

Figure 1: An example of a galaxy at $z = 0.48$ is shown with its Keck LRIS slit position, the observed emission line and the measured and model rotation curve. Note that any underestimate of the rotational velocity will lead to an *overestimate* of the brightening! The Tully-Fisher relation derived from such measurements is shown in Vogt *et al.* (1997) and Vogt & Phillips (this volume).

and morphological attributes were determined for 140 galaxies from the HST HDF images. Of this sample, redshifts were ultimately determined for 115 galaxies (now available on the web). Further measurements such as rotation curves, velocity widths and line ratios were made for subsets of these galaxies.

2.1 Tully-Fisher at Intermediate Redshift

In a recently published paper using HST data largely from the high latitude WFPC GTO field (the "Groth" strip), Vogt *et al.* (1996) demonstrated that it was possible to combine measurements from HST WFPC2 images with ground-based Keck multislit observations at moderate spectral resolution to derive rotational velocities for suitablly-inclined spiral galaxies to redshifts $z \sim 1$ (see Figure 1). Based on a comparison of the velocity widths in these nine galaxies with the local Tully-Fisher (TF) relations, a limit of $\Delta M_B < 0.6$ mag could be set on the brightening at intermediate redshift. The more recent Tully-Fisher work on the disk/spiral galaxy sample in the HDF in Vogt *et al.* (1997; see also Vogt & Phillips, this volume) greatly improves the reliability of this estimate, first by adding a comparable number of galaxies, and second, adding galaxies of lower absolute luminosity. The distant galaxy TF relation is now much more clearly defined, and provides the strongest evidence to date for modest evolutionary brightening of $\Delta M_B \sim 0.4$ at $<z> \sim 0.5$.

2.2 Nature of Compact Galaxies: I.

One of the striking results of HST images of faint, distant field galaxies has been the prevalance of compact, relatively high surface brightness galaxies (with effective radii r_e typically $0.2''$-$0.3''$). Our early work on CNELGs (compact narrow emission line galaxies – Koo *et al.* 1995; Guzmán *et al.* 1996) showed that these objects had kinematical, structural and photometric properties comparable to the more extreme examples at the current epoch of low mass, active star forming galaxies, the HII galaxies. But the question remained for the more typical objects – "what are the current-day analogues of the compact galaxies seen at redshifts $0.3 \lesssim z \lesssim 1$?"

This question was addressed in two parts. First, Phillips *et al.* (1997; see also Koo *et al.* – this volume) used the HST HDF images to derive sizes, magnitudes and morphologies. These were then combined with the Keck redshifts to derive luminosities and length scales. They are luminous, with median $M_B \sim -20$ (H_0 = 50 km s^{-1} Mpc^{-1}). The Keck spectra also yielded velocity widths (σ), allowing us to estimate their masses. The velocity widths ranged from $\sigma < 35$ km s^{-1} (the measurement limit) to 150 km s^{-1}. Combined, these data allowed us to compare and characterize the high redshift compact sample (see Figure 2). While a small fraction appear to be ellipticals, the vast majority are emission-line galaxies whose global properties resemble nearby HII galaxies, i.e., compact, late-type, star forming galaxies.

2.3 Nature of Compact Galaxies: II.

The second aspect, the spectroscopic properties of the emission-line "compact" sample galaxies, is discussed in Guzmán *et al.* (1997). Star formation rates were derived from measurements of the [OII] equivalent widths; these ranged from 5Å to 95Å. The corresponding star formation rates are <1-15 $M_\odot$ yr^{-1} (based on procedures and calibrations given in Guzmán *et al.*). Based on all the available data, namely velocity widths, excitations, Hβ luminosities, star formation rates, and M/L estimates, a substantial fraction of these "compact" emission-line galaxies ($\sim 60\%$) appear to be like local, low mass, extreme star forming HII galaxies. The remainder are actively star forming, but appear to be a more heterogeneous sample of late-type galaxies.

An interesting result of this effort is that some additional constraints can be now placed on the evolution of the star formation rate per unit volume with redshift (see Figure 3 and the discussion in Guzmán *et al.* 1997). The data are consistent with a large decline in the SFR from $z \sim 1$ to the present epoch.

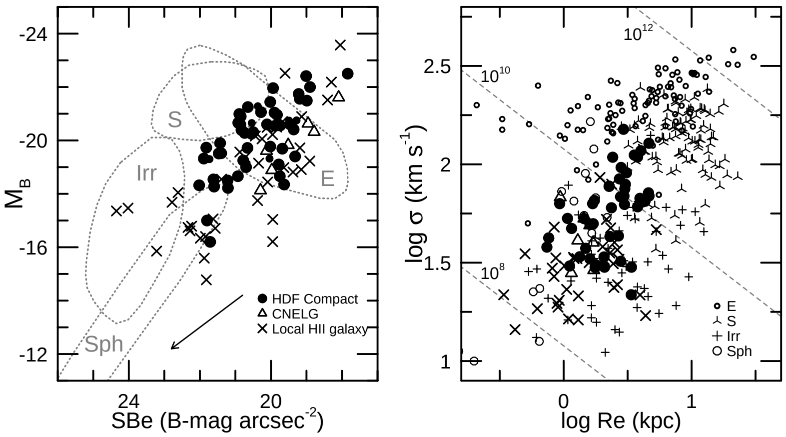

Figure 2: The luminosity-surface brightness relation for local samples of galaxies with the high redshift "compact" sample overplotted, on the left panel, from Phillips *et al.* (1997). The right panel again shows the relationship of the distant sample with local samples in the velocity width (σ)–effective radius plane. Typical masses are indicated. The "compact" objects are the filled circles. The properties of the high redshift galaxies overlap those of local, late-type galaxies.

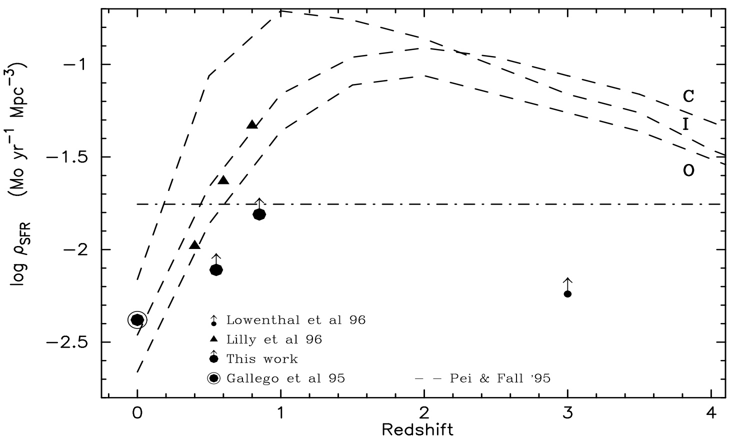

Figure 3: Estimates of the star formation rate per unit volume at several redshifts (from Guzmán *et al.* 1997). The sources are given on the figure. Models (closed, infall and outflow) from Pei and Fall (1995) are shown, as is the average at -1.75 derived from the local luminosity density (from Madau *et al.* 1996). Note that "compact" galaxies make a substantial contribution at intermediate redshifts, and that the SFR decline from $z \sim 1$ to the current epoch is large – a factor $\sim$10.

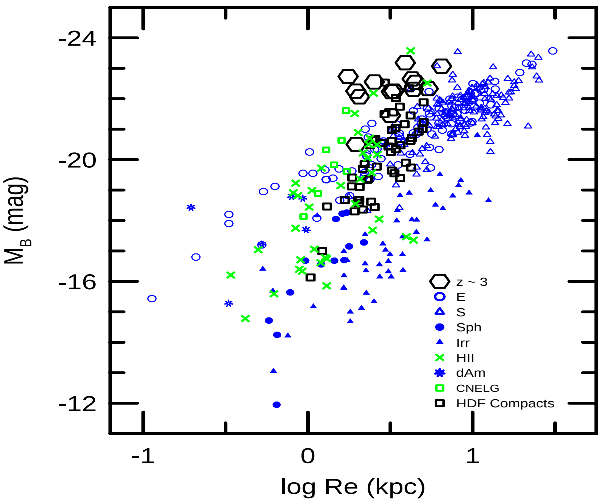

Figure 4: The location of the high redshift sample in the $M_B - r_e$ plane, compared to local galaxies (Lowenthal *et al.* 1997; see also this volume). The large symbols are the $z \sim 3$ galaxies. Even though they are very luminous, the high redshift galaxies do overlap with the local, bright, star forming HII galaxies. A key issue is whether the high redshift objects have comparable velocity widths (and hence masses).

2.4 Galaxies at very High Redshift

The use of U-band "dropout" galaxies to identify potential high redshift objects was beautifully exemplified by Steidel *et al.* (1996a) in their spectroscopic observations from Keck. This was followed by one of the very first HDF papers utilizing spectroscopic data (Steidel *et al.* 1996b); they found 5 high redshift ($z \sim 3$) galaxies. The "dropout" technique relies upon the large flux decrements that occur from line-of-sight and source absorption as both Lyα and the Lyman-limit pass through the filter bandpass. Decrements in the U-band relative to other filters typically indicate sources at redshifts $z \gtrsim 2.5$, while decrements in the B-band suggest even higher redshift sources ($z \gtrsim 3$).

This technique, applied through the use of both U and B-band "dropout" objects, was the means by which we selected a sample of 24 galaxies for observation at Keck with LRIS. Of this sample 11 were confirmed to have redshifts in the range $2.2 < z < 3.4$. The remaining galaxies, with one exception, are consistent with being high redshift objects, but could not be confirmed spectroscopically. The high redshift objects in the HDF are quite small, but

luminous ($1.8 < r_{\frac{1}{2}} < 6.5 h_{50}^{-1}$ kpc and $-21.5 < M_B < -23$), and show a wide diversity of forms. Interestingly, they are not as morphologically uniform as the brighter sample studied by Giavalisco *et al.* (1996).
Combining these new data with the 5 in the HDF from Steidel *et al.* (1996b), we have derived co-moving volume densities and star formation rates (Lowenthal *et al.* 1997; this volume also). It is striking that these HDF data already indicate that the volume density is comparable to the local volume density of all galaxies brighter than L* (and 3-4× higher than the first estimate of Steidel *et al.* (1996a) based on a brighter sample of "dropout" candidates. If the remaining objects in the original "dropout" sample prove to be at high redshift, the co-moving volume density could be several times higher still. Star formation rates have been estimated from the rest-frame UV continuum fluxes. They are found to be typical of local HII galaxies and many spiral galaxies (at $6 - 27 h_{50}^{-2}$ M$_\odot$ yr^{-1} for $q_0 = 0.5$, or $2 - 9 h_{50}^{-2}$ M$_\odot$ yr^{-1} for $q_0 = 0.05$).

Acknowledgments

Funding was provided by the CfPA (Center for Particle Astrophysics) and by NSF grants AST-91-20005, and AST-9529098, and NASA grants AR-6337.08-94A, AR-6337.21-94A, GO-5994.01-94A, AR-5801.01-94A, and AR-6402.01-95A.

References

1. Gallego, J. *et al.*, ApJ, 455, L1, 1995.
2. Giavalisco, M. *et al.*, ApJ, in press, 1996.
3. Guzmán, R. *et al.*, ApJ, 460, L5, 1996.
4. Guzmán, R. *et al.*, ApJ, submitted, 1997.
5. Koo, D. C. *et al.*, ApJ, 440, L49, 1995.
6. Lilly, S. J. *et al.*, ApJ, 460, L1, 1996.
7. Lowenthal, J. D. *et al.*, ApJ, submitted, 1997.
8. Madau, P. *et al.*, MNRAS, in press, 1996.
9. Pei, Y. C. & Fall, S. M., ApJ, 464, 69, 1995.
10. Phillips, A. C. *et al.*, ApJ, submitted, 1997.
11. Steidel, C. C. *et al.*, ApJ, 462, L17, 1996a.
12. Steidel, C. C. *et al.*, ApJ, in press, 1996b.
13. Vogt, N. P. *et al.*, ApJ, submitted, 1997.
14. Vogt, N. P. *et al.*, ApJ, 465, L15, 1996.
15. Williams, R. *et al.*, AJ, in press, 1996.